calculations are currently being repeated using Eq. (4), and it is expected that accurate fine grid solutions can be achieved.

Acknowledgment

This work was supported by a grant to the second author from the Natural Sciences and Engineering Research Council of Canada. The authors wish to thank J. B. Malone for his comments, which have improved the discussion contained herein, and Denis Jones from the National Aeronautical Establishment for his valuable suggestions, which have contributed to the success of this formulation.

References

[1]Barron, R. M., and Naeem, R. K., "Numerical Solution of Transonic Flows on a Streamfunction Co-ordinate System," *International Journal for Numerical Methods in Fluids,* Vol. 9, No. 10, 1989, pp. 1183-1193.

[2]Hafez, M., Murman, E. M., and South, J., "Artificial Compressibility Methods for Numerical Solution of the Transonic Full Potential Equation," AIAA Paper 78-1148, July 1978.

[3]Naeem, R. K., "Computation of Transonic Flows Using a Streamfunction Coordinate System," Ph.D. Dissertation, University of Windsor, Windsor, Ontario, Canada, 1988.

[4]Murman, E. M., and Cole, J. D., "Calculation of Plane Steady Transonic Flows," *AIAA Journal,* Vol. 9, No. 1, 1971, pp. 114-121.

[5]Garabedian, P. R., and Korn, D., "Analysis of Transonic Airfoils," *Communications of Pure and Applied Mathematics,* Vol. 24, 1971, pp. 841-851.

[6]Sinclair, P. M., "An Exact Integral (Field Panel) Method for the Calculation of Two Dimensional Transonic Potential Flow around Complex Configurations," *Aeronautical Journal,* Vol. 25, No. 896, 1986, pp. 227-236.

[7]Jameson, A., and Yoon, S., "Lower-Upper Implicit Schemes with Multiple Grids for the Euler Equations," *AIAA Journal,* Vol. 25, No. 7, 1987, pp. 929-935.

[8]Wigton, L. B., "Application of MACSYMA and Sparse Matrix Technology to Multielement Airfoil Calculations," AIAA Paper 87-1142, 1987.

General Purpose Program to Generate Compatibility Matrix for the Integrated Force Method

J. Nagabhusanam*
Indian Institute of Science, Bangalore, India
and
S. N. Patnaik†
NASA Lewis Research Center, Cleveland, Ohio

Introduction

THE novel formulation termed the "integrated force method" (IFM) has been established in recent years for analysis, and design of structures.[1-8] In the integrated force method of analysis, a structure idealized by finite elements is designated as "structure (n,m)" where (n,m) are the force and displacement degrees of freedoms of the discrete model, respectively. The structure (n,m) has m equilibrium equations and $r=(n-m)$ compatibility conditions. The generation of the equilibrium equation is straightforward. The generation of the compatibility condition is intricate. We have introduced the concepts to generate compatibility conditions in Refs. 5 and 6. The earlier work was confined to 1) field compatibility conditions only and 2) structure types considered were limited to frame works and plates but not their combinations. The distinct features of this Note from earlier publications are 1) both field and boundary compatibility conditions are examined, 2) different element types are used in the finite element idealization, and 3) a key feature termed "node determinancy" has been introduced. The node determinancy concept enables elimination of nodes of a discrete model at the intermediate stage of the generation of compatibility conditions, which in turn reduces the complexity of the deformation displacement relations. This process enhances computational efficiency.

The two key equations of IFM are Eq. (1) calculation of forces, and Eqs. (2), calculation of displacements of a structure (n,m)[1,3]:

$$\begin{bmatrix} [B] \\ [C][G] \end{bmatrix} F = \begin{Bmatrix} P \\ \text{------} \\ \delta R \end{Bmatrix} \qquad \text{or,} \qquad [S]\{F\} = \{P\}^* \tag{1}$$

where $[B]$ is the $(m\times n)$ equilibrium matrix, $[C]$ the $(r\times n)$ compatibility matrix, $[G]$ the $(n\times n)$ concatenated flexibility matrix, $\{P\}$ the m-component load vector, $\{\delta R\}$ the r-component effective initial deformation vector, $\{\delta R\} = -[C]\{\beta_0\}$, where, $\{\beta_0\}$ is the n-component initial deformation vector, and $[S]$ the $(n\times n)$ governing matrix.

Displacements $\{X\}$ are obtained from the forces $\{F\}$ by back substitution:[3]

$$\{X\} = [J]\{[G]\{F\} + [\beta_0]\} \tag{2a}$$

where $[J]$ is the $(m\times n)$ deformation coefficient matrix defined as

$$[J] = m \text{ rows of } [[S]^{-1}]^T \tag{2b}$$

In this Note, the generation of the compatibility matrix $[C]$ is presented in brief.

Strain Formulation of St. Venant

The strain formulation of St. Venant is illustrated taking the example of a plane stress elasticity problem. The strain displacement relations of the problem can be written as

$$\epsilon_x = \frac{\partial u}{\partial x}, \quad \epsilon_y = \frac{\partial v}{\partial y}, \quad \gamma_{xy} = \frac{\partial u}{\partial y} + \frac{\partial v}{\partial x} \tag{3}$$

In Eq. (3), three strain components (ϵ_x, ϵ_y, and γ_{xy}) are expressed in terms of two displacements (u, v).Thus, there is a constraint on strains, which is obtained by the elimination of the displacements. This constraint is the compatibility condition, which has the following form:

$$\frac{\partial^2 \epsilon_x}{\partial y^2} + \frac{\partial^2 \epsilon_y}{\partial x^2} - \frac{\partial^2 \gamma_{xy}}{\partial x \partial y} = 0 \tag{4}$$

The two steps of strain formulation of elasticity are as follows:

Step 1. Establish the strain displacement relations [Eq. (3)].

Step 2. Eliminate displacements from Eq. (3) to obtain the compatibility condition, Eq. (4).

Compatibility Conditions of Finite Element Analysis

St. Venant's fomulation for elastic continua has been extended to finite element analysis to generate discrete compatibility conditions. In the first step, the deformation displacement relations of a finite element analysis (which are

Received June 6, 1988; revision received May 18, 1989.

*Associate Professor.

†Senior NRC Fellow.

analogous to the strain displacement relations of elasticity) are obtained as[5]:

$$\{\beta\} = [B]^T\{X\} \tag{5}$$

In Eq. (5), n deformations $\{\beta\}$ of an indeterminant structure (n,m) for which $(n>m)$, are expressed in terms of its m displacements $\{X\}$. Elimination of the m displacements from the n deformation displacement relations given by Eq. (5) yields the $r=n-m$ compatibility conditions and the associated compatibility matrix $[C]$ of dimension $(r\times n)$ as:

$$[C]\{\beta\} = \{0\} \tag{6}$$

The principal steps to generate the compatibility matrix $[C]$ are as follows:

Step 1. Pick an element from the finite element model and any one of its deformations, β_1 for example. Establish its bandwidth.[4,5] Let the deformations of all the elements within the region of influence defined by the bandwidth constitute set S_1. Segregate the deformation displacement relation which belongs to set S_1 and designate these relations as DDR_0.

Step 2. Eliminate displacements from relations DDR_0 to generate one compatibility condition. Reduce the number of relations in DDR_0 by one by dropping any one deformation displacement relation that has participated in the compatibility condition. The reduced deformation displacement relation designated as DDR_1 can be symbolized as

$$\{\beta\}^{(1)} = [B]^{(1)T}\{X\} \tag{7}$$

In Eq. (7), deformation $\{\beta\}^{(1)T}$ is a $(n-1)$ component vector, dimension of matrix $[B]^{(1)T}$ is $\{(n-1)\times m\}$, and DDR_1 contains $r-1=n-m-1$ compatibility conditions.

Step 3. Node determinancy condition: Since the number of deformations is equal to the number of forces, dropping a deformation β_t is equivalent to the elmination of the corresponding force component F_t. Take, for example, a node i. Let K_i represent the number of forces present in the equilibrium equation at the node i. Let L_i represent the displacement degrees of freedom of the node i, which also represents the number of equilibrium equations at that node. The indeterminancy of the node i designated NR_i is defined as

$$NR_i = K_i - L_i \tag{8}$$

If $NR_i = 0$, then i is determinate. Forces or deformations present at determinate node i do not participate in the compatibility conditions since such forces can be determined from the nodal equilibrium equations alone. Consequently, for determinate node i, K_i forces or deformations along with $L_i = K_i$ displacements can be dropped simultaneously from the deformation displacement relation DDR_1 without affecting the compatibility conditions in any manner. Dropping displacements and deformations is equivalent to the elimination of appropriate columns and rows in the deformation displacement relations DDR_1. The reduced deformation displacement relation obtained after imposing the node determinancy condition designated DDR_2 has the following form:

$$\{\beta\}^{(2)} = [B]^{(2)T}\{X\}^{(2)} \tag{9}$$

In Eq. (9), the matrix $[B]^{(2)T}$ has dimension $\{(n-1-K_i)\times(m-K_i)\}$. The deformation vector $\{\beta\}^{(2)}$ has dimension $(n-1-K_i)$ and displacements $\{X\}^{(2)}$ are of dimension $(m-K_i)$. As expected, the number of compatibility conditions contained in DDR_2 given by Eq. (9) is as follows:

$$r_2 = \{(n-1-K_1)-(m-K_i)\} = (r-1)$$

since only one compatibility condition has been generated. The node determinancy condition has reduced the number of deformation displacement relations from $(r-1)$ to $(r-1-K_i)$; however, the number of compatibility conditions remains the same. The motivation for eliminating determinate deformation variables (which is equivalent to elimination of determinate forces) after the generation of a compatibility condition is to enhance "node determinancy" at as many nodes as possible. Following steps 2 and 3, all of the compatibility conditions contained in S_1 (DDR_0) are obtained.

Step 4. Repeat steps 1–3 until all $r=n-m$ compatibility conditions in the field and on the boundary are generated from the structure (n,m).

A computer program has been developed to generate compatibility conditions primarily based on these four steps. The matrix operations are carried out utilizing matrix sparsities and a central memory block is used to store matrices and vectors. The program forms a module of the IFM finite-element code, and it is written in Fortan IV language.

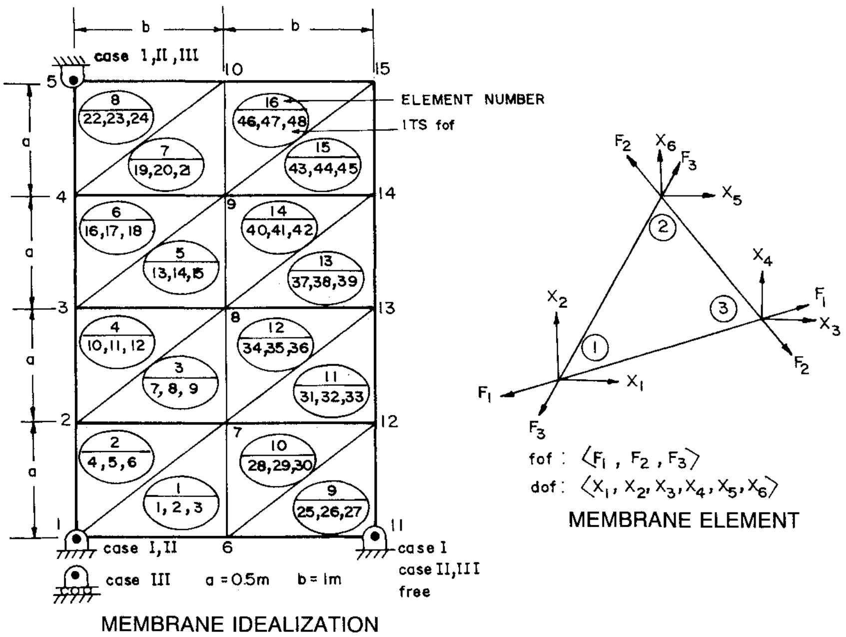

Fig. 1 Two-bay membrane.

Illustrative Example

The compatibility conditions, as obtained from the computer program, are illustrated taking the example of a rectangular membrane shown in Fig. 1. The membrane is discretized by 16 triangular membrane elements and has 15 nodes. The element has three force variables (F_1, F_2, F_3). Its nodal displacements are $(X_1, X_2, ..., X_6)$ as depicted in Fig. 1. Three sets of boundary conditions are considered for the problem.

Boundary condition Case I: Nodes (1,5,11) are fully restrained. The membrane (48,24) has $(r=n-m=24)$ compatibility conditions.

Boundary condition Case II: Nodes (1,5) are fully restrained. The membrane (48,26) has $(r=n-m=22)$ compatibility conditions.

Boundary condition Case III: Node 5 is fully restrained while node 1 is partially restrained. This membrane (48,27) has $(r=48-27=21)$ compatibility conditions.

The compatibility conditions (CC_1 to CC_{24}) as given by Eqs. (10) for the membrane boundary case I, obtained from the computer program, are separated into three groups for discussion: Group I—Interface Compatibility Conditions; Group II—Cluster Compatibility Conditions; Group III—Boundary Compatibility Conditions. The compatibility conditions have the following explicit form

Group I: Interface Compatibility Conditions

CC_1:

$$-\beta_5+\beta_7=0 \tag{10a}$$

connecting elements 2 and 3 (Fig. 2)

CC_2:

$$-\beta_2+\beta_{30}=0 \tag{10b}$$

connecting elements 1 and 10 (Fig. 2)

CC_3:

$$-\beta_{29}+\beta_{31}=0 \tag{10c}$$

connecting elements 10 and 11 (Fig. 2)

CC_4:

$$-\beta_{27}+\beta_{28}=0 \tag{10d}$$

connecting elements 9 and 10 (Fig. 2)

CC_5:

$$\beta_{33}-\beta_{34}=0 \tag{10e}$$

connecting elements 11 and 12 (Fig. 2)

CC_6:

$$\beta_3-\beta_4=0 \tag{10f}$$

connecting elements 1 and 2 (Fig. 2)

CC_7:

$$-\beta_8+\beta_{36}=0 \tag{10g}$$

connecting elements 3 and 12 (Fig. 2)

CC_8:

$$-\beta_9+\beta_{10}=0 \tag{10h}$$

connecting elements 3 and 4 (Fig. 2)

CC_9:

$$-\beta_{35}+\beta_{37}=0 \tag{10i}$$

connecting elements 12 and 13 (Fig. 2)

CC_{10}:

$$-\beta_{39}+\beta_{40}=0 \tag{10j}$$

connecting elements 13 and 14 (Fig. 2)

CC_{11}:

$$-\beta_{11}-\beta_{13}=0 \tag{10k}$$

connecting elements 4 and 5 (Fig. 2)

CC_{12}

$$-\beta_{14}+\beta_{42}=0 \tag{10l}$$

connecting elements 5 and 9 (Fig. 2)

CC_{13}

$$-\beta_{15}+\beta_{16}=0 \tag{10m}$$

connecting elements 5 and 6 (Fig. 2)

CC_{14}

$$-\beta_{41}+\beta_{43}=0 \tag{10n}$$

connecting elements 14 and 15 (Fig. 2)

CC_{15}

$$-\beta_{45}+\beta_{46}=0 \tag{10o}$$

connecting elements 15 and 16 (Fig. 2)

CC_{16}

$$\beta_{17}-\beta_{19}=0 \tag{10p}$$

connecting elements 6 and 7 (Fig. 2)

CC_{17}

$$-\beta_{20}+\beta_{48}=0 \tag{10q}$$

connecting elements 7 and 16 (Fig. 2)

CC_{18}

$$-\beta_{21}+\beta_{22}=0 \tag{10r}$$

connecting elements 7 and 8 (Fig. 2).

Group II: Compatibility Conditions

CC_{19}

$$-0.4472\beta_1+0.8944\beta_2+\beta_4+0.4472\beta_5-0.8944\beta_6 +0.8944\beta_8-\beta_9-\beta_{27}+0.4472\beta_{29}-0.8944\beta_{32}+\beta_{34} -0.4472\beta_{35}=0 \quad \text{(lower cluster)} \tag{10s}$$

CC_{20}

$$-0.4472\beta_{13}+0.8944\beta_{14}+\beta_{16}-0.8944\beta_{18}+0.4472\beta_{19}$$
$$+0.8944\beta_{20}-\beta_{21}\beta_{40}+0.4472\beta_{41}-0.8944\beta_{44}$$
$$+\beta_{46}-0.4472\beta_{47}=0 \qquad \text{(upper cluster)} \qquad (10t)$$

CC_{21}

$$-0.4472\beta_{7}+0.8944\beta_{8}+\beta_{10}-0.8944\beta_{12}+0.4472\beta_{13}$$
$$+0.8944\beta_{14}-\beta_{15}-\beta_{34}+0.4472\beta_{35}-0.8944\beta_{38}$$
$$+\beta_{40}-0.4472\beta_{41}=0 \qquad \text{(middle cluster)} \qquad (10u)$$

Group III: External or Boundary Compatibility Conditions

CC_{22}

$$\beta_6+\beta_{12}+\beta_{18}+\beta_{24}=0 \qquad (10v)$$

connecting elements 2, 4, 6, 8

CC_{23}

$$\beta_1+\beta_{25}=0 \qquad (10w)$$

connecting elements 1-9

CC_{24}

$$0.8944\beta_1-\beta_4+2.683\beta_6-0.4472\beta_7-2.683\beta_8+\beta_{10}$$
$$+1.789\beta_{12}-0.4472\beta_{13}-1.789\beta_{14}+\beta_{16}+0.8944\beta_{18}$$
$$-0.4472\beta_{19}-0.8944\beta_{21}-0.4472\beta_{23}-1.789\beta_{26}+2\beta_{28}$$
$$-1.789\beta_{30}-0.8944\beta_{31}=0 \qquad (10x)$$

connecting elements 1,2,3,...,11.

Membrane boundary case II: This structure differs from boundary case I with respect to release of two restraints at node 11. Two releases reduce two external compatibility conditions, which can be identified as CC_{23} and C_{24}. Membrane boundary case II has 22 compatibility conditions (CC_1 to CC_{22}). Membrane boundary case III: This structure has three boundary restraints, and it represents an externally determinate structure. The structure has no external compatibility conditions, its 21 field compatibility conditions; are CC_1 to CC_{21}.

Interpretation of the Compatibility Conditions

Group I: Interface Compatibility Conditions

The interface constraints (CC_1 to CC_{18}) link deformations of two neighboring elements. Take for example CC_{10}; this condition links deformations β_{39} of element 13 to deformation β_{40} of its neighboring element 14 as $\beta_{39}=\beta_{40}$ along the common nodes 8-14 of the two elements (refer to Fig. 2). The interface compatibility conditions of the structure are symbolized as (MM) and are depicted in Fig. 2.

Group II: Cluster Compatibility Conditions

In a finite element model a cluster is defined as a series of adjoining elements. The cluster compatibility condition represents a constraint on the deformations of the elements that belong to the cluster. For the membrane there are three clusters, referred to as lower, upper, and middle clusters, as shown Fig. 2. The three constraints (CC_{19}, CC_{20}, and C_{21}) represent the cluster compatibility conditions.

Group III: External or Boundary Compatibility Conditions

For the membrane boundary case I, six displacements are restrained, however only three conditions are sufficient for its kinematic stability. Thus, the structure has three boundary in-

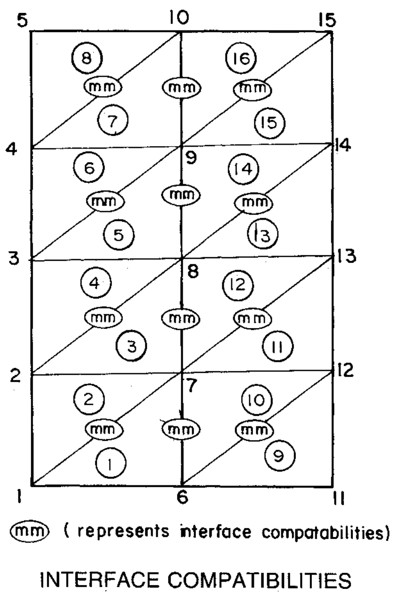

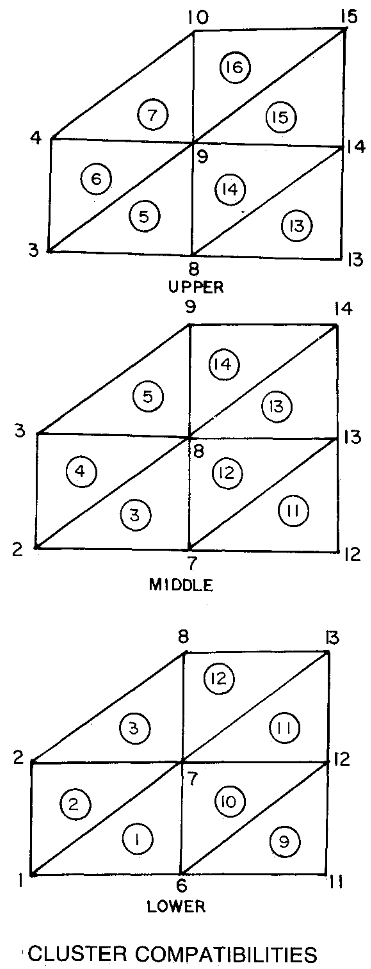

Fig. 2 Compatibility conditions for two-bay membrane.

determinancies, which give rise to three external or boundary compatibility conditions (CC_{22}, CC_{23}, and CC_{24}). The CC_{22} establishes deformation conformity between boundary nodes (1-5), likewise CC_{23} and CC_{24} constrains deformations along nodes (1,6,11) and nodes (5,4,3,2,1,6, and 11), respectively.

Discussion

Bandwidth of Compatibility Conditions

The upper bound to the bandwidth of compatibility conditions for a finite element model is ascertained from the location of elements in the discretization. For example, for the membrane shown in Fig. 1, the deformations of element 1, has to be compatible with its neighboring elements such as elements (1,2,3,9,10,11,12), which have been referred to as the lower cluster. The cluster consists of seven elements; each element has three force degrees of freedoms. The force degrees of freedom of the cluster is ($7 \times 3 = 21$). The maximum number of entries in any compatibility condition which belongs to this cluster is 21, which represents the upperbound bandwidth. The actual bandwidth of an individual compatibility condition is usually much smaller than its upperbound bandwidth. The lower cluster has eight compatibility conditions, (CC_1, CC_2,...,CC_7 and CC_{19}). The upperbound bandwidth of 21 represents the composite bandwidth of all of the eight compatibility conditions of the cluster.

Upperbound Bandwidth of External Compatibility Conditions

The bandwidth of external compatibility conditions is examined taking the example of membrane boundary case I. Consider the elements (including their influencing elements) along the path connecting two or more boundary nodes. Let *EBW* represent the force degrees of freedom of all the elements along the path of the boundary nodes. The upperbound bandwidth of the external compatibility conditions is equal to *EBW*. Like the field compatibility conditions, the actual bandwidth of external compatibility condition is also much smaller than their upper bounds. The three external compatibility conditions (CC_{22},CC_{23},CC_{24}) have (4,2,19) entries respectively.

Computation Time

Computation time required to generate compatibility conditions for several structures are reported in Ref. 5. Here a rule of thumb is provided to estimate the upper and lower bounds to the computations required to generate the compatibility conditions. Consider a structure (n,m), and let the upper bound to the bandwidth of the $r = n - m$ compatibility conditions be represented by $(\gamma_1,\gamma_2,\ldots,\gamma_r)$ and actual bandwidths obtained be represented as $(\delta_1,\delta_2,\ldots,\delta_r)$. Let the total computational time required to solve r sets of linear equations of dimensions $(\gamma_1,\gamma_2,\ldots,\gamma_r)$ be represented by T_U. Likewise, time for the same when equation dimensions are changed to $(\delta_1,\delta_2,\ldots,\delta_r)$ be (T_L). The bounds to the computation time to generate the compatibility conditions of the structure are as follows:

$$\text{Upperbound time} = T_U \qquad \text{Lowerbound time} = T_L \tag{11}$$

Only the upperbound time T_U can be estimated before the generation of the compatibility conditions. The lowerbound time T_L, which represents a more realistic estimation, cannot be acertained a priori, since the actual bandwidths of compatibility conditions are known only after their generation. However, for a structure with many thousands of degrees of freedoms, the upperbound time T_U itself rerpresents a minor fraction of total computations required for the solution of the problem.

Conclusion

The generation of both field and boundary compatibility conditions from deformation displacement relations utilizing two key features: 1) compatibility bandwidth and 2) the node determinancy concept represents an efficient procedure to obtain the compatibility conditions of finite element models. The computer program generates sparse and banded compatibility conditions for a structure idealized by finite elements. The program requires no more additional input data than that is required by the finite element stiffness method. The bandwidth information and node determinancy condition are generated internally. We belive that the principle behind the generation of the compatibility conditions for finite element analysis, by and large, has been completed.

References

[1]Patnaik, S. N., "An Integrated Force Method for Discrete Analysis," *International Journal of Numerical Methods in Engineering*, Vol. 6, No. 2, 1973, pp. 237-251.

[2]Patnaik, S. N., "The Variational Energy Formulation for the Integrated Force Method," *AIAA Journal*, Vol. 24, Jan. 1986, pp. 129-137.

[3]Patnaik, S. N., "Integrated Force Methods versus the Standard Force Method," *International Journal of Computers and Structures*, Vol. 22, 1986, pp. 151-163.

[4]Patnaik, S. N. and Yadgiri, S., "Frequency Analysis of Structures by Integrated Force Method," *Journal of Sound and Vibration*, Vol. 83, No. 1, 1982, pp. 93-109.

[5]Patnaik, S. N. and Joseph, K. T., "Generation of the Compatibility Matrix in the Integrated Force Method," *Jnl. Comp. in Appl. Mech. and Engrg.*, Vol. 55, 1986, pp. 239-257.

[6]Patnaik, S. N. and Joseph, K. T., "Compatibility Conditions from Deformation Displacement Relations," *AIAA Journal*, Vol. 23, 1985, pp. 1291-1293.

[7]Patnaik, S. N. and Gallagher, R. H., "Gradients of Behavior Constraint from Deformation Displacement Relations," *International Journal of Numerical Methods in Engineering*, Vol. 23, 1986, pp. 2205-2215.

[8]Patnaik, S. N. and Yadgiri, S., "Design for Frequency by the Integrated Force Method," *Comp. Meth. in Appl. Mech. and Engrg.*, Vol. 16, 1978, pp. 213-230.

Accurate Bending Analysis of Laminated Orthotropic Plates

S. Savithri* and T. K. Varadan†
Indian Institute of Technology, Madras, India

Introduction

MANY advances have been made in the theoretical development of higher-order theories for composite plates to account for shear deformation. A careful examination of the three-dimensional elasticity solution by Pagano[1] for a bidirectional composite plate reveals the nonlinearity of inplane displacements u and v in any layer with respect to thickness coordinate, as well as a sudden change of their slopes at the interfaces between two layers. By comparison with elasticity solution, Bert[2] evaluated different refined plate theories and concluded that a discrete layer version of a higher-order theory should be accurate.

Discrete layer theories proposed earlier incorporate either the slope discontinuity at an interface[3] or the nonlinear variation of u and v[4], but not both. Further they have the number of unknown variables increasing with the number of layers, thus making the analysis costly for practical laminates.

Received May 30, 1989; revision received Nov. 14, 1989.

*Research Scholar, Department of Mathematics.

†Professor, Department of Aerospace Engineering.